Estimating hydraulic conductivity from drainage patterns—A case study in the Oregon Cascades

Wei Luo[1,*], Bartosz P. Grudzinski[1], and Darryll Pederson[2]
[1]Department of Geography, Northern Illinois University, DeKalb, Illinois 60115, USA
[2]Department of Geosciences, University of Nebraska–Lincoln, Lincoln, Nebraska 68588-0340, USA

ABSTRACT

This study introduces a new method for estimating hydraulic conductivity based on the concept of effective groundwater drainage length and DuPuit-Forchheimer assumptions. The effective groundwater drainage length is related to the surface drainage dissection patterns (as expressed in drainage density) forming over long periods of time. Application of the new method to the Oregon Cascades yielded hydraulic conductivity values similar to those documented in the literature. This method represents an effective and efficient way of estimating hydraulic conductivity for regions where the interplay among surface drainage, groundwater, and topography has established a steady-state dynamic equilibrium. It also provides a theoretically sound approach for extrapolating limited local measurements to a large region and revealing the spatial variation of hydraulic conductivity.

INTRODUCTION

Hydraulic conductivity K is a key parameter in hydrology that describes the ease at which fluid moves through a porous media (e.g., Freeze and Cherry, 1979; Deming, 2002). As part of Darcy's Law, K is fundamental in quantifying groundwater flow systems. K often exhibits a large range of variability (up to several orders of magnitude), even for the same type of rock (Freeze and Cherry, 1979). It is traditionally measured by conducting pumping tests in the field (Hornberger et al., 1998) or estimated based on field measurements of quantities such as discharge, heat flow, etc., coupled with computer modeling (e.g., Ingebritsen et al., 1992, 1994). These methods often prove to be expensive, time consuming, and impractical for remote areas.

The interaction between surface water and groundwater is well known (e.g., Dunne, 1990; Freeze, 1987). In general, regions with less permeable surface materials are often associated with higher drainage density (D) and attributed to higher surface runoff potential (Strahler, 1964; DeVries, 1976). Pederson (2001) further pointed out that drainage patterns often carry the imprint of groundwater systems since headward extension is often aided by groundwater sapping and/or seepage weathering because of higher and directional groundwater gradients at channel heads. Numerous studies have used empirical equations to correlate various drainage basin parameters in terms of surface runoff (e.g., Jaeger et al., 2007; Montgomery and Dietrich, 1989; Dietrich et al. 1993; Vogt et al., 2003). However, groundwater is addressed only in terms of infiltration as it limits surface runoff, whereas our study considers the consequences of the infiltrating water. We introduce an innovative method of estimating K from drainage dissection patterns based on the concept of effective drainage length and a dynamic equilibrium condition under DuPuit-Forchheimer assumptions. The drainage dissection pattern as expressed in D can be derived from digital elevation model (DEM) data. Application of this method to the Oregon Cascades yielded K values similar to those documented in the literature. This method represents a more effective and efficient way of estimating K than the traditional methods for regions where a steady-state dynamic equilibrium exists between surface water and groundwater.

METHODOLOGY

Figure 1 shows a simplified conceptual model, consisting of a river channel and an aquifer that discharges into the channel. The assumptions are that (1) the aquifer is effectively drained (i.e., a steady-state dynamic equilibrium has developed over a long time), and (2) groundwater flow is primarily horizontal (i.e., Dupuit-Forchheimer assumptions apply). The aquifer thickness is H [L], the valley depth is d [L], and the effective drainage length is W [L]. The datum is considered to be the base of the aquifer. At a distance W from the river, the zone of saturation intercepts the land surface. W is unique for specified hydrologic parameters K, R, d, and H (see Fig. 1). If the aquifer is not effectively drained, more surface area away from the channel will be saturated, which will generate more runoff. The increased runoff will increase recharge rates for the stretch of aquifer labeled W (Fig. 1). This will increase groundwater gradients and cause the river bank to become unstable and susceptible to weathering and erosion. Bank instabilities will continue until channel migration and/or the development of new tributaries has produced the D required to effectively drain the area of the aquifer discharging to the channel and a dynamic equilibrium between recharge and discharge is reached (Freeze, 1987; Pederson, 2001). W is thus called the effective drainage length.

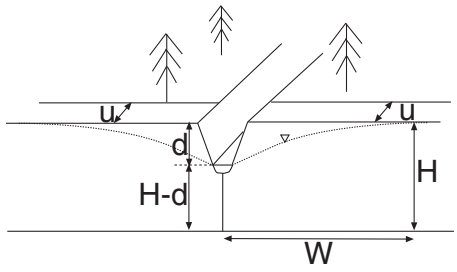

Figure 1. Diagram illustrating conceptual model for deriving *K* from drainage dissection patterns. See text for details. (Note derivation does not require surface to be saturated at *x* = *W*, as long as *H* can be properly estimated.)

Using Dupuit-Forchheimer assumptions and a modification of Deming's equation (2002) to incorporate our concept, the discharge per unit length ($u = 1$) of the channel q' [L^2T^{-1}] is:

$$q' = \frac{1}{2}K\left(\frac{H^2-(H-d)^2}{W}\right). \quad (1)$$

Rearranging Equation 1 to solve for K [LT^{-1}] leads to:

$$K = \frac{2q'W}{H^2-(H-d)^2}. \quad (2)$$

STUDY AREA AND PARAMETER ESTIMATES

We chose the Cascade Range, Oregon (see Fig. 2A for location), to test the method because this area has a sharp contrast in D (Tague and Grant, 2004; Luo and Stepinski, 2008), K has been documented in the literature (Ingebritsen et al., 1992, 1994; Manga, 1996, 1997; Saar and Manga, 2004; Gannett and Lite, 2004; Conlon et al., 2005; Jefferson et al., 2006), and D has been derived from DEM data (Luo and Stepinski, 2008). The study area has two prominent regions: the Western Cascades and the High Cascades, both of which formed by the subduction of the Juan de Fuca plate under the North American plate (Jefferson et al., 2006). Rift-related volcanism has resulted in the eruption of dominantly basaltic and andesitic lavas over the last 5 m.y. (Conrey et al., 2002). The Western Cascades are underlain by older (Tertiary age), lower-permeability volcanic rocks of varying

*E-mail: wluo@niu.edu.

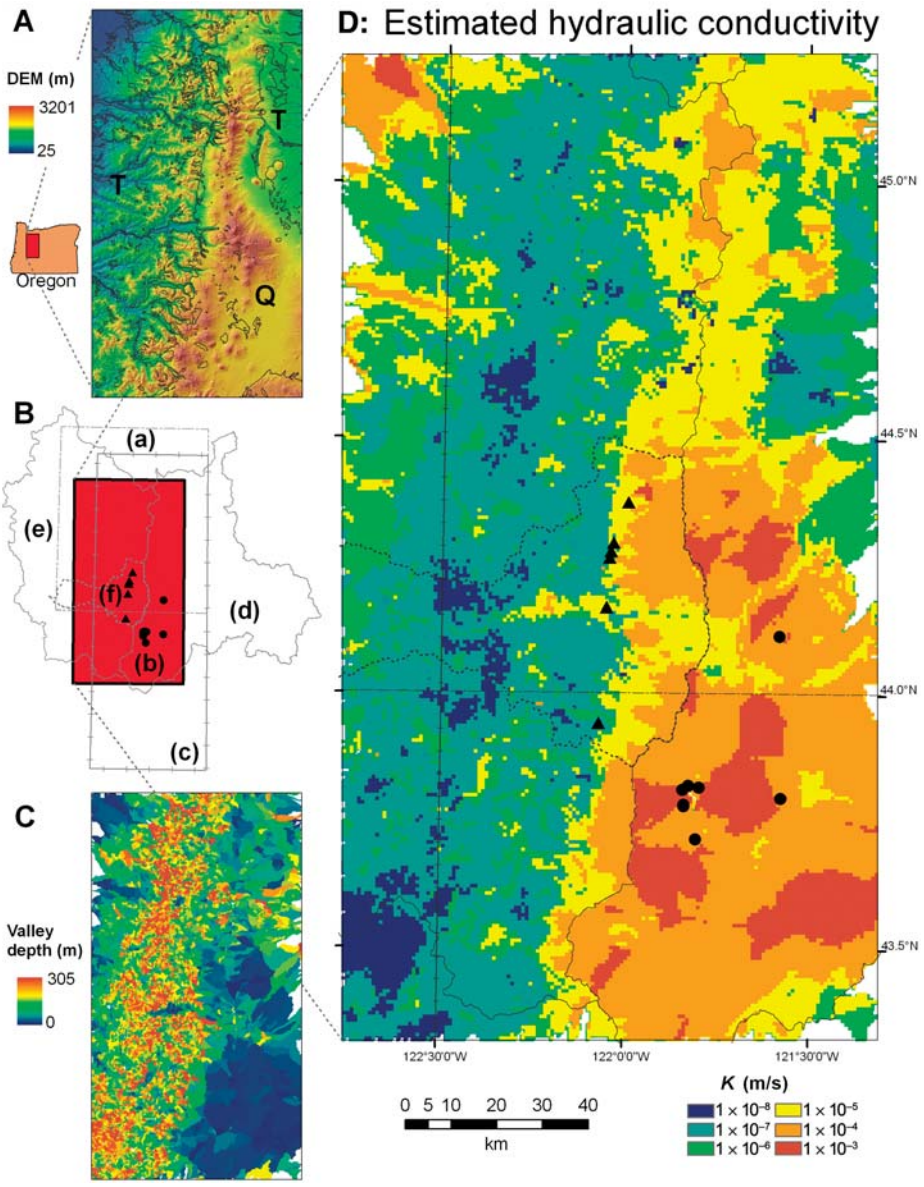

Figure 2. (A) Shaded relief map of study area derived from digital elevation model (DEM) data, obtained from U.S. Geological Survey National Elevation Data Set with 37.315 m resolution (min = 24.8 m, max = 3200.8 m, mean = 1023.1 m, std dev. = 481.0 m). Also shown are simplified geologic age boundaries (Walker and MacLeod, 1991): T—Tertiary, Q—Quaternary. Study area location coordinates are 121.31°W to 122.75°W and 43.31°N to 45.26°N. (B) Labels a–f refer to approximate boundaries or well/spring locations of previous studies as summarized in Table 1. Red shading shows our study area. (C) Valley depth *d* by watershed estimated using Black Top Hat transformation method (min = 0 m, max = 305.2 m, mean = 68.2 m, std dev. = 56.3 m). (D) Spatial distribution of estimated *K* by orders of magnitude. Lines, black dots, and triangles show boundaries or well/spring locations of previous studies (see also part B; Table 1). (A very small percentage of cells is negative, and at the order of 1 × 10^{-2} m/s, and are thus not shown for clarity; see Fig. 3.)

compositions and are highly dissected, whereas the High Cascades are underlain by young (mostly Quaternary age), higher-permeability volcanic rocks having a relatively uniform composition and a much smoother surface (Walker and MacLeod, 1991; Jefferson et al., 2006). The Western Cascades landscape is characterized by lower elevation, higher relief, and higher *D* than the High Cascades (Tague and Grant, 2004; Fig. 2A). These differences are partly attributed to differences in age and volcanism (Tague and Grant, 2004), among other things, such as permeability of rocks. The *K* values documented in the literature for these regions are summarized in Table 1, and their approximate locations are shown in Figure 2B. The basaltic aquifers in the two regions are characterized by joints and fractures, which provide pathways for groundwater movement; and because the basalts formed during periodic volcanic eruptions, heterogeneities exist in aquifer parameters. However, these heterogeneities are limited in areal and vertical extent and will not influence the overall main drainage patterns that cover much larger areas.

In Equation 2, q' can be estimated from precipitation (p [LT^{-1}]) and infiltration rate (i [%, dimensionless]), assuming a dynamic equilibrium condition, i.e., recharge from precipitation (applied to the unit length on both sides of the channel) is equal to the discharge into the channel:

$$q' = p \times i \times (2Wu) / u = 2p \times i \times W. \quad (3)$$

For p, we used the mean annual precipitation acquired from the PRISM spatial climate data set, which is spatially variable (with a resolution of ~800 m) (PRISM Group, Oregon State University, http://www.prismclimate.org, created 4 February 2004). The value of i is taken to be 30% of precipitation for the Western Cascades (Conlon et al., 2005) and 50% for the High Cascades (Ingebritsen et al., 1992).

We estimated d from DEM data using the Black Top Hat (BTH) transformation, which is a gray-level morphologic image analysis tool (Rodriguez et al., 2002). More details can be found in Soille (2003). Operationally, the BTH transformation first finds the maximum elevation from the present-day DEM within a circle centered on a target cell and stores the maximum value as the output for the target cell. The process is repeated until all the cells of the DEM are processed. The result of this step is called dilation. Next, the dilation result is subject to a similar moving-window process, but this time to find the minimum value within the circle. The result is called closing, which represents the DEM of a pre-incision surface. The final BTH result is obtained by subtracting the present-day DEM from the pre-incision DEM. The intersection between BTH result and channel network line is the estimate of d. The radius of the moving circle was set to 500 m by comparing different results with manually measured depths from the DEM at selected sites. Since d changes along the channel, we used the average value of d within the watershed that drains into each channel (see Fig. 2C). All other variables and results were also averaged by watershed. It should be recognized that there is downcutting of the channel over time, but with a landscape in dynamic equilibrium, the area surrounding the channel is also likely lowering, and thus change in d should be minimal.

We derived W from D, which was computed from DEM data (Luo and Stepinski, 2008) as a continuous raster based on the downslope flow length from a given cell to its nearest channel (Tucker et al., 2001); the channel networks were extracted from DEM using a morphology-based algorithm that extracts networks conforming to the observed dissection patterns (Molloy and Stepinski, 2007):

TABLE 1. ESTIMATES OF *K* (IN M/S) DOCUMENTED IN THE LITERATURE

Reference	Min	Max	Accepted order of magnitude	Location label in Figure 2B	Method
Ingebritsen (1992, 1994)*	3×10^{-7}	1×10^{-5}		(a)	Groundwater flow, heat flow, computer modeling
Manga (1996, 1997)†			10^{-5}	(b)	Spring flow, computer model
Saar and Manga (2004)§	3×10^{-6}	1×10^{-2}	10^{-6}	(c)	Spring flow, heat flow, hydroseismicity, magma intrusion
Gannett and Lite (2004)#	3×10^{-5}	1×10^{-3}	10^{-5}	(d)	Literature, computer model
Conlon et al. (2005)	7×10^{-8}	7×10^{-4}		(e)	Wells, literature
Jefferson et al. (2006)	3×10^{-4}	1×10^{-2}	10^{-3}	(f)	Spring, isotope, model

*These values are converted from permeability estimates assuming a water temperature of 5 °C for near-surface conditions, consistent with well-test data from shallow (<50 m) domestic wells in Western Cascades (McFarland, 1983).
†The order of magnitude is inferred for young (<2 Ma) volcanic rocks (also converted from permeability).
§These values are for near-surface conditions and horizontal *K*. The accepted order of magnitude is for the upper 500 m.
#The accepted order of magnitude is for the upper 457 m (1500 ft) of material in the High Cascades area of the Deschutes Basin.

$$W = 1/(2D). \quad (4)$$

H is estimated to be 500 m for the Western Cascades (Conlon et al., 2005) and 100 m for the High Cascades (Jefferson et al., 2006).

K is calculated at the watershed level, and Equation 2 becomes:

$$K = \frac{p \times i}{D^2[H^2 - (H-d)^2]}. \quad (5)$$

RESULTS AND DISCUSSION

Figure 2D presents the spatial distribution of *K* estimated in the study area at watershed level. There is a large variability in *K* across the study area. The results show the contrast in *K* between the Western Cascades, ranging from 10^{-8} to 10^{-6} m/s, and the High Cascades, ranging from 10^{-5} to 10^{-2} m/s. The results are also generally consistent in orders of magnitude with previous studies (see Table 1 and Fig. 3, and Fig. 2B for location). About two thirds of our study area falls within the study areas of Ingebritsen et al. (1992, 1994), and the range of our estimate of *K* (10^{-8}–10^{-5} m/s) generally matches their results (10^{-7}–10^{-5} m/s) for the Western Cascades. A majority of our study area coincides with the study area of Saar and Manga (2004). Their estimated *K* (in horizontal direction and near-surface conditions) ranges from 10^{-6} to 10^{-2} m/s, again consistent with our overall range of the whole study area (10^{-8}–10^{-2} m/s). Manga (1996, 1997) estimated *K* to be on the order of 10^{-5} m/s based on spring discharge measurements and computer modeling. Our estimates at the spring locations range from 10^{-5} to 10^{-3} m/s. The computer simulation of Gannett and Lite (2004) in the upper Deschutes basin yielded *K* values ranging from 10^{-5} to 10^{-3} m/s, the same as our estimate in that general area. Jefferson et al. (2006) studied the groundwater flow patterns on the west slope of the High Cascades and found *K* to be 3×10^{-4} to 1×10^{-2} m/s, consistent with our estimate for the High Cascades. Conlon et al. (2005) conducted detailed well tests of the Willamette Basin and found *K* to range from 7×10^{-8} to 7×10^{-4} m/s, exactly matching our estimated order of magnitude for the Western Cascades. In addition, the boundary between $K = 10^{-7}$ m/s and higher values generally outlines the geologic age boundary between Tertiary and Quaternary rocks. Furthermore, unlike the traditional methods that can only derive *K* values for local sites, our method is able to derive *K* over the whole study area, revealing spatial variations.

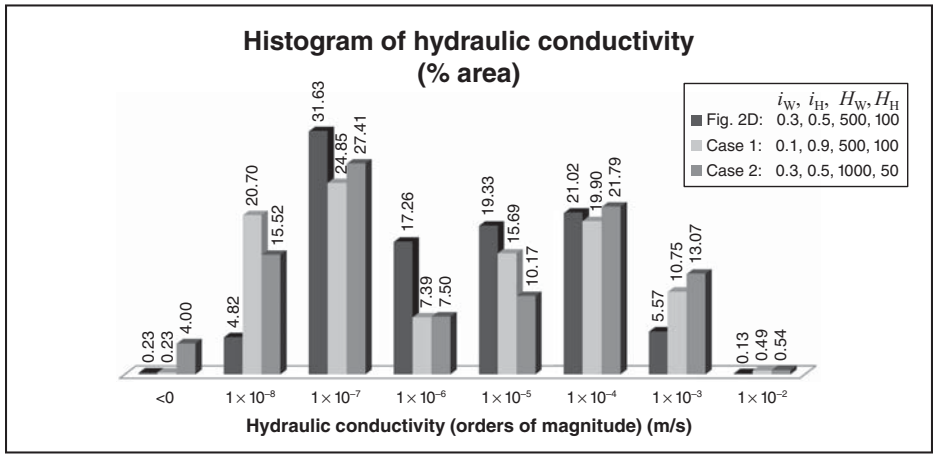

Figure 3. Histogram of estimated *K* by orders of magnitude as shown in Figure 2D and two other cases. See text for discussion.

The assumptions of our method mean that it is best suited for regions where the interplay among surface drainage, groundwater, and topography has established a steady-state dynamic equilibrium (e.g., the study area). This could be achieved over long periods of time (e.g., on the order of m.y.) by (1) headward groundwater sapping, (2) seepage weathering followed by subsequent surface-water erosion, or (3) simple adjustment of the groundwater system to surface topography over time, or some combinations of these. The main stream valleys and overall drainage pattern of such areas should carry the imprint of the groundwater gradient and would reflect the macroscale properties of the aquifer rather than local heterogeneities. In addition, the method can only be used to estimate near-surface horizontal *K*. However, *K* for deeper aquifers can be estimated using the exponential or power-law decay with depth (e.g., Saar and Manga, 2004). The dynamic equilibrium condition is reasonable because we are dealing with drainage dissection patterns that take a very long time to develop and respond very slowly to changes in climate, base level, or tectonics, etc. While surface water can be very erosive, the eroding surface is likely made more susceptible to erosion by long-term groundwater seepage weathering (Pederson, 2001). Mean values of precipitation and infiltration are appropriate to use because they are more important in long-term dynamic equilibrium conditions. Paleoclimatic studies based on paleosols of central Oregon show that the range of changes in mean annual precipitation for the past 40 m.y. (Retallack et al., 2000; Sheldon et al., 2002) is similar to the variance within PRISM data. These variations of the past climate are not expected to make significant changes to our estimate of *K*, especially in orders of magnitude.

The parameters *D* and *d* are reasonably constrained from DEM data. To test the sensitivity of the method to variations in parameter estimates, we evaluated different combinations of values for *i* and *H*. The results all have similar spatial patterns as shown in Figure 2D and similar orders of magnitude as documented in

the literature, but have different spatial extent for each order of magnitude. Two scenarios are reported here. In case 1, H is kept the same as the base case (Fig. 2D), but i is set to 10% and 90% for Western and High Cascades, respectively. This scenario results in an overall decrease in K for the Western Cascades and an overall increase in the High Cascades as compared with the result in Figure 2D (see Table 2). In case 2, i is kept the same as the base case, but H is set to 1000 m and 50 m for the Western and High Cascades, respectively. This scenario also shows an overall decrease in K for the Western Cascades and an increase in the High Cascades as compared with the base case (Table 2). If $H^2 - (H - d)^2 < 0$, or $2H < d$, K will become negative, which is meaningless. (This is also shown in Fig. 3 for case 2.) So $2H > d$ can be used as a constraint to set a proper value for H if no other constraint is available. Overall, the sensitivity tests show that our method produces the general spatial pattern and orders of magnitude in K as documented in the literature, and changes up to a factor of 3 in i and one order of magnitude in H would not significantly alter the result except the percentage of area in each order of magnitude.

In summary, we present a new method for estimating K based on the concept of effective drainage length and a dynamic equilibrium condition under DuPuit-Forchheimer assumptions. The effective drainage length is associated with D, which can be derived from DEM data. The parameters used to calculate K can be reasonably constrained from DEM data and previous studies. Application of our method to the study area of the Oregon Cascades yielded K values similar to those documented in the literature. This method represents an effective and efficient way of estimating K, and it is especially beneficial for areas where human testing is not practical. This method also provides a theoretically sound approach for extrapolating limited local measurements to a large region and revealing the spatial variation of K.

ACKNOWLEDGMENTS

We thank two anonymous reviewers for their thorough and helpful reviews. This research is partially supported by NASA grant NNX08AM98G to Luo.

REFERENCES CITED

Conlon, T.D., Wozniak, K.C., Woodcock, D., Herrera, N.B., Fisher, B.J., Morgan, D.S., Lee, K.K., and Hinkle, S.R., 2005, Ground-Water Hydrology of the Willamette Basin, Oregon: U.S. Geological Survey Scientific Investigations Report 2005–5168, 83 p.

Conrey, R.M., Taylor, E.M., Donnely-Nolan, J.M., and Sherrod, D.R., 2002, North-central Oregon Cascades: Exploring petrologic and tectonic intimacy in a propagating intra-arc rift, *in* More, G.W., ed., Field Guide to Geologic Processes in Cascadia: Oregon Department of Geology and Mineral Industries Special Paper 36, p. 47–90.

Deming, D., 2002, Introduction to Hydrogeology: New York, McGraw-Hill, 480 p.

DeVries, J.J., 1976, The groundwater outcrop-erosion model; evolution of the stream network in The Netherlands: Journal of Hydrology (Amsterdam), v. 29, p. 43–50, doi: 10.1016/0022-1694(76)90004-4.

Dietrich, W.E., Wilson, C.J., Montgomery, D.R., and McKean, J., 1993, Analysis of erosion thresholds, channel networks, and landscape morphology using a digital terrain model: The Journal of Geology, v. 101, no. 2, p. 259–278, doi: 10.1086/648220.

Dunne, T., 1990, Hydrology, mechanics, and geomorphic implications of erosion by subsurface flow, *in* Higgins, C.G., and Coates, D.R., eds., Groundwater Geomorphology: The Role of Subsurface Water in Earth-Surface Processes and Landforms: Geological Society of America Special Paper 252, p. 1–28.

Freeze, R.A., 1987, Modeling interrelationships between climate, hydrology, and hydrogeology and the development of slopes, *in* Anderson, M.G., and Richards, K.S., eds., Slope Stability: New York, John Wiley & Sons, p. 381–403.

Freeze, R.A., and Cherry, J.A., 1979, Groundwater: Englewood Cliffs, New Jersey, Prentice-Hall, 604 p.

Gannett, M.W., and Lite, K.E., Jr., 2004, Simulation of Regional Ground-Water Flow in the Upper Deschutes Basin, Oregon: U.S. Geological Survey Water Resources Investigations Report 03–4195, 84 p.

Hornberger, G., Raffensperger, J., Wilberg, J., and Eshleman, K., 1998, Elements of Physical Hydrology: Baltimore, Maryland, John Hopkins University Press, 302 p.

Ingebritsen, S.E., Sherrod, D.E., and Mariner, R.H., 1992, Rates and patterns of groundwater flow in the Cascade Range volcanic arc, and the effects on subsurface temperatures: Journal of Geophysical Research, v. 97, p. 4599–4627, doi: 10.1029/91JB03064.

Ingebritsen, S.E., Mariner, R.H., and Sherrod, D.R., 1994, Hydrothermal Systems of the Cascade Range, North Central Oregon: U.S. Geological Survey Professional Paper 1044-L, 86 p.

Jaeger, K.L., Montgomery, D.R., and Bolton, S.M., 2007, Channel and perennial flow initiation in headwater streams: Management implications of variability in source-area size: Environmental Management, v. 40, p. 775–786, doi: 10.1007/s00267-005-0311-2.

Jefferson, A., Gordon, G., and Rose, T., 2006, Influence of volcanic history on groundwater patterns on the west slope of the Oregon High Cascades: Water Resources Research, v. 42, p. W12411, doi: 10.1029/2005WR004812.

Luo, W., and Stepinski, T., 2008, Identification of geologic contrasts from landscape dissection pattern: An application to the Cascade Range, Oregon, USA: Geomorphology, v. 99, p. 90–98, doi: 10.1016/j.geomorph.2007.10.014.

Manga, M., 1996, Hydrology of spring-dominated streams in the Oregon Cascades: Water Resources Research, v. 32, p. 2435–2439, doi: 10.1029/96WR01238.

Manga, M., 1997, A model for discharge in spring-dominated streams and implications for transmissivity and recharge of Quaternary volcanic in the Oregon Cascades: Water Resources Research, v. 33, p. 1813–1822, doi: 10.1029/97WR01339.

McFarland, W.D., 1983, A description of aquifer units in Western Oregon: U.S. Geological Survey Open File Report 82–165, 35 p.

Molloy, I., and Stepinski, T.F., 2007, Automatic mapping of valley networks on Mars: Computers & Geosciences, v. 33, p. 728–738, doi: 10.1016/j.cageo.2006.09.009.

Montgomery, D.K., and Dietrich, W.E., 1989, Source areas, drainage density, and channel initiation: Water Resources Research, v. 25, no. 8, p. 1907–1918, doi: 10.1029/WR025i008p01907.

Pederson, D.T., 2001, Stream piracy revisited: A groundwater sapping solution: GSA Today, v. 11, no. 9, p. 4–10, doi: 10.1130/1052-5173(2001)011<0004:SPRAGS>2.0.CO;2.

Retallack, G.J., Bestland, E.A., and Fremd, T.J., eds., 2000, Eocene and Oligocene Paleosols of Central Oregon: Geological Society of America Special Paper 344, 192 p.

Rodriguez, F., Maire, E., Courjault-Rade, P., and Darrozes, J., 2002, The Black Top Hat function applied to a DEM: A tool to estimate recent incision in a mountainous watershed (Estibère watershed, central Pyrenees): Geophysical Research Letters, v. 29, doi: 10.1029/2001GL014412.

Saar, M.O., and Manga, M., 2004, Depth dependence of permeability in the Oregon Cascades inferred from hydrogeologic, thermal, seismic, and magmatic modeling constraints: Journal of Geophysical Research, v. 109, p. B04204, doi: 10.1029/2003JB002855.

Sheldon, N.D., Retallack, G.J., and Tanaka, S., 2002, Geochemical climofunctions from North American soils and application to paleosols across the Eocene-Oligocene boundary in Oregon: The Journal of Geology, v. 110, p. 682–696, doi: 10.1086/342865.

Soille, P., 2003. Morphological Image Analysis: Principles and Applications (2nd ed.): New York, Springer-Verlag, 391 p.

Strahler, A.N., 1964, Quantitative geomorphology of drainage basins and channel networks, *in* Ven Te Chow, ed., Handbook of Applied Hydrology: New York, McGraw Hill, p. 4-39–4-76.

Tague, C., and Grant, G.E., 2004, A geological framework for interpreting the low flow regimes of Cascade streams, Willamette River Basin, Oregon: Water Resources Research, v. 40, p. W04303, doi: 10.1029/2003WR002629.

Tucker, G.E., Catani, F., Rinaldo, A., and Bras, R.L., 2001, Statistical analysis of drainage density from digital terrain data: Geomorphology, v. 36, p. 187–202, doi: 10.1016/S0169-555X(00)00056-8.

Vogt, J.V., Colombo, R., and Bertolo, F., 2003, Deriving drainage networks and catchment boundaries: A new methodology combining digital elevation data and environmental characteristics: Geomorphology, v. 53, p. 281–298, doi: 10.1016/S0169-555X(02)00319-7.

Walker, G.W., and MacLeod, N.S., 1991, Geologic Map of Oregon; Special Geologic Map: Reston, Virginia, U.S. Geologic Survey, 2 sheets, 1:500,000 scale.

TABLE 2. STATISTICS AND SENSITIVITY TEST OF K (IN M/S) USING DIFFERENT i AND H

	Figure 2D (i_W, i_H, H_W, H_H) (0.3, 0.5, 500, 100)		**Case 1 (i_W, i_H, H_W, H_H) (0.1, 0.9, 500, 100)**		**Case 2 (i_W, i_H, H_W, H_H) (0.3, 0.5, 1000, 50)**	
	West Cas.	High Cas.	West Cas.	High Cas.	West. Cas.	High Cas.
MEAN	2.49×10^{-6}	6.83×10^{-4}	8.28×10^{-7}	1.23×10^{-3}	1.26×10^{-6}	1.28×10^{-3}
STD	8.99×10^{-6}	1.01×10^{-2}	3.00×10^{-6}	1.83×10^{-2}	4.68×10^{-6}	1.62×10^{-2}

Note: Subscripts W and H indicate values for Western Cascades and High Cascades.

Manuscript received 27 October 2009
Revised manuscript received 3 November 2009
Manuscript accepted 6 November 2009

Printed in USA